

Supporting information for:

Influence of the Debye length on the interaction of a small molecule-modified Au nanoparticle with a surface-bound bioreceptor

Natalia Bukar^a, Sandy Shuo Zhao^a, David M. Charbonneau^{a,b}, Joelle N. Pelletier^{a,b,c}, Jean-Francois Masson^{a,d*}

^a Département de chimie, Université de Montreal, C.P. 6128 Succ. Centre-Ville, Montreal, Qc, Canada, H3C 3J7

^b PROTEO

^c Centre de Chimie Verte et Catalyse (CCVC)

^d Centre for self-assembled chemical structures (CSACS)

Materials and Methods

Materials

2-amino-2-hydroxymethyl-propane-1,3-diol (Tris), 2-(N-morpholino)ethanesulfonic acid (MES), NaH₂PO₄, Na₂HPO₄ were purchased from Merck. NaCl, NaOH were purchased from Sigma-Aldrich, USA. Gold trichloride trihydrate and sodium citrate dihydrate were purchased from Fisher Scientific. All buffers were prepared using deionized water (18 MΩ/cm resistance, Direct-Q from Millipore). Folic acid (Sigma-Aldrich) was dissolved in 0.1 M Na₂HPO₄ adjusted with 0.05 M NaOH to pH 7 and quantified using a Cary 100 Bio UV/Vis Spectrometer ($\epsilon_{282} = 27.0 \text{ mM}^{-1} \text{ cm}^{-1}$). MTX was dissolved in 0.05 M KOH and quantified in 0.1 M NaOH ($\epsilon_{258} = 22.1 \text{ mM}^{-1} \text{ cm}^{-1}$ and $\epsilon_{302} = 23.3 \text{ mM}^{-1} \text{ cm}^{-1}$). The enzyme human dihydrofolate reductase (hDHFR) was expressed recombinantly in *Escherichia coli* and purified following a two-step purification protocol described by Volpato *et al.*¹

Preparation of folic acid-functionalized gold nanoparticles

Gold nanoparticles (Au NP) were prepared by reducing chloroauric acid to neutral Au with sodium citrate ². Briefly, the Au NP were prepared by mixing a 50 mL of 1 mM solution of gold trichloride trihydrate solution in purified water and 2 mL of a 2 % w/v solution of sodium citrate dihydrate, also prepared in purified water. The mixture was stirred under boiling conditions for 10 minutes, and then, for 10 minutes at room temperature to form Au NP stabilized with citrate. The average Au NP diameter of 13 nm was estimated using UV-Vis spectra ³.

Folic acid-functionalized gold nanoparticles (FA Au NP) were synthesized following the procedure established by Zhao *et al.* ⁴. Briefly, 0.5 mL of a freshly prepared aqueous solution of 80 μ M folic acid was added to 4.5 mL of the Au NP solution at a concentration of 1 nM. The mixture was stirred for 20 minutes shielded from light, and then, centrifuged at 12 000 g for 20 minutes. The supernatant with excess folic acid was carefully removed and the pellet was resuspended in the buffer solutions. The concentration of FA Au NP was estimated using UV/Vis spectra ³.

Determination of enzymatic activity of hDHFR

Kinetic assays were conducted for different buffer compositions at 20°C to monitor the reduction of 5,6-dihydrofolate (DHF) to 5,6,7,8-tetrahydrofolate in a nicotinamide adenine dinucleotide phosphate (NADPH)-dependent reaction catalyzed by hDHFR¹. Substrates were dissolved in the buffer and quantified by spectrophotometry (ϵ_{340} = 6200 M⁻¹ cm⁻¹ for NADPH and ϵ_{282} = 28,400 M⁻¹ cm⁻¹ for DHF) using a Cary 100 Bio UV/Vis spectrophotometer (Varian Canada Inc., Montréal, QC). Kinetic parameters for the hDHFR were determined by monitoring the depletion of 100 μ M NADPH and 100 μ M DHF ($\Delta\epsilon_{340}$ = 12,800 M⁻¹ cm⁻¹). All results are an average of three independent experiments. Units of enzyme activity were calculated from a non-linear regression fit to the Michaelis-Menten

equation using Graphpad Prism (Graphpad Software, San Diego, CA) and according to the protein concentration determined by the Bradford assay (BioRad).

Aggregation assay

The aggregation kinetics were measured from the fraction of Au NP remaining in solution at different time intervals. The UV-Vis absorption spectra were taken for freshly prepared solutions of FA Au NP, and for these solutions after different storage times, on a Cary 100 Bio UV-Vis Spectrometer (Varian Canada, Inc., Montreal, QC). The samples were sonicated for 1 minute before the measurements. The absorbance at the resonance wavelength served to calculate the fraction of free particles in solution. Aggregation constants were calculated after 10 days as explained in the main text.

SPR sensing

SPR measurements to quantify the interaction of FA Au NP and hDHFR in different buffers were carried out with a home-built SPR system, as previously described by Bolduc *et al.* ⁵. Briefly, the SPR sensors were prepared by cleaning 22 x 22 mm glass slides with piranha solution. *Caution, piranha solution is very corrosive!* Then, a 5 nm Cr adhesion layer and a 50 nm Au film were deposited on the glass slide. The Au surface was reacted overnight with a 2 mg/mL solution of 3-MPA-LHDLHD prepared in DMF. The monolayers were then reacted with N α ,N α -bis(carboxymethyl)-L-lysine as described elsewhere ⁶. This monolayer was competent to bind copper ions and then, His-tagged hDHFR ⁶.

The interaction of the FA Au NP with hDHFR in presence of MTX was measured in the following conditions: 100 nM MTX and 0.25 nM FA Au NP dissolved in different buffers (See Table SI1). A baseline of the SPR sensorgram was measured for 5 minutes in the same buffer as for the analysis. The FA Au NP and MTX solution was injected on the SPR for 20 minutes to record the magnitude of the SPR signal. The difference of the SPR response for

solutions of 0 and 100 nM MTX evaluated the sensitivity of the assay in each buffer. Larger SPR responses correlated with improved interactions between the FA Au NP and hDHFR.

Mapping the surface electrostatic potential of hDHFR

The pH titration curve was determined for hDHFR (PDB code: 1DHF) using the MOE software (Molecular Operating Environment (MOE2006.02), and its titration module. The following parameters were used for calculation: ionic strength = 20 mM sodium phosphate buffer (44 mM NaCl equivalent), the dielectric constant of water (78) and the viscosity of water at 25°C (0.89 mPa s). The protein model did not contain any detectable hydrogen atoms since the crystal structure resolution was 2.30 Å. The hydrogens were added by simulating the protonation at pH 7 and defined as the starting point for calculating the pK_a of each side chain using the PROPKA program⁷. The protonation state was then evaluated at each pH (taking into account the pK_as) and the net charge calculated. The titration curve is shown in Fig SI2. The calculated isoelectric point (pI) based on the structure was 8.27. Based on the simulated titration, a net charge (formal charge) of +4 was calculated at pH 6, and +0.5 at pH 8.

The surface electrostatic potential was calculated using the adaptive Poisson-Boltzmann solver (APBS) in PyMOL. The Poisson-Boltzmann equation is described as follows (c.g.s unit system):

$$\vec{\nabla}[\epsilon(\vec{r})\vec{\nabla}\psi(\vec{r})] = -4\pi\rho^f(\vec{r}) - 4\pi\sum_i c_i^\infty z_i q \exp\left(\frac{-z_i q \psi(\vec{r})}{kT}\right) \lambda(\vec{r})$$

where $\vec{\nabla}$ is the divergence operator, $\epsilon(\vec{r})$ represents the position-dependent dielectric constant, $\vec{\nabla}\psi(\vec{r})$ represents the gradient of the electrostatic potential, $\rho^f(\vec{r})$ represents the charge density of the solute, c_i^∞ represents the concentration of ion i at an infinite distance from the molecule, z_i is its valency, q is the charge of a proton, k is the Boltzmann

constant, T is the temperature, and $\lambda(\vec{r})$ describes the accessibility to ion at point \vec{r} . If the potential is not large compared to kT , the equation can be linearized to be solved more efficiently, leading to the Debye-Hückel equation⁸.

The surface electrostatic potential is expressed as kT/e where e is the charge of an electron. The protein isocontours were generated and the surface electrostatics mapped onto the electronic density map on the protein surface. The potentials were set as $\pm 3 kT/e$. The exterior surface (the entrance) of the binding pocket is mainly positively charged. These positive charges are contributed by arginine and lysine residues surrounding the entrance of the binding pocket.

Table SI1. Activity measurement of hDHFR in several buffers

<i>Buffer</i>	<i>Activity, U/mg</i>	<i>%CV *</i>
Tris 100 mM, pH 8	11.5	2
Tris 50 mM, pH 8	7.9	1
Tris 10 mM, NaCl 154 mM, pH 8	18.2	4
MES 100 mM, pH 8	4.4	1
MES 10 mM, pH 8	4.0	7
PB 100 mM, pH 8	4.6	4
PB 50 mM, pH 8	4.9	3
PB 10 mM, pH 8	6.0	2
PB 10mM, NaCl 17 mM, pH 8	6.9	4
PB 10mM, NaCl 154 mM, pH 8	8.2	2
PB 10mM, NaCl 308 mM, pH 8	17.9	3
PBS 1X, pH 8	11.2	4
PB 100 mM, pH 6	4.1	5

* The coefficient of variation (%CV) was measured for a triplicate SPR measurement.

Table SI2. SPR, Debye length and aggregation data for different buffer compositions

<i>Buffer</i>	<i>K_{10d} (M⁻¹ s⁻¹)</i>	<i>% aggregated > 1 month</i>	<i>Debye length - κ^{-1} (nm)</i>	<i>SPR $\Delta \lambda_{max}$ * (nm)</i>	<i>SPR %CV**</i>
Tris 100 mM	2 x 10 ⁴	82 ± 2%	0.74	0.23	8
Tris 50 mM			1.0	0.11	6
Tris 10 mM, NaCl 154 mM	2 x 10 ⁵	95 ± 2%	0.57	0	2
MES 100 mM	9 x 10 ²	66 ± 3%	0.74	0.05	2
MES 10 mM			2.3	0.08	2
PB 100 mM	3 x 10 ³	40 ± 1%	0.74	0.49	7
PB 50 mM	1 x 10 ³	15 ± 1%	1.0	0.31	8
PB 10 mM			0.74	0.12	2
PB 10mM, NaCl 17 mM	2 x 10 ³	33 ± 2%	0.68	0.11	3
PB 10mM, NaCl 154 mM	6 x 10 ³	45 ± 2%	0.46	0.46	5
PB 10mM, NaCl 308 mM	9 x 10 ³	90 ± 3%	0.36	0.60	8
PBS 1X	8 x 10 ³	62 ± 1%	0.45	0.62	8

* Difference between the λ_{max} shift of binding of 100 nM hDHFR to 0.25 nM FA-AuNP and the λ_{max} shift of binding of 100 nM hDHFR to 0.25 nM FA-AuNP in the presence of 100 nM MTX in the solution.

** The coefficient of variation (%CV) was measured for a triplicate SPR measurement.

Table SI3. Ionic strength of 0.1 M phosphate buffer for varying pH, and stability of Au NP solutions in different buffers (13 nm Au NP)

<i>pH</i>	<i>IS, M</i>	<i>SPR $\Delta \lambda_{max}$ * (nm)</i>	<i>%CV**</i>
8.0	0.29	0.78	15
7.5	0.27	0.8	7
7.0	0.22	0.76	6
6.5	0.16	0.68	7
6.0	0.12	2.52	2

* Difference between the λ_{max} shift of binding of 100 nM hDHFR to 0.25 nM FA-AuNP and the λ_{max} shift of binding of 100 nM hDHFR to 0.25 nM FA-AuNP in the presence of 100 nM MTX.

** The coefficient of variation (%CV) was measured for a triplicate SPR measurement.

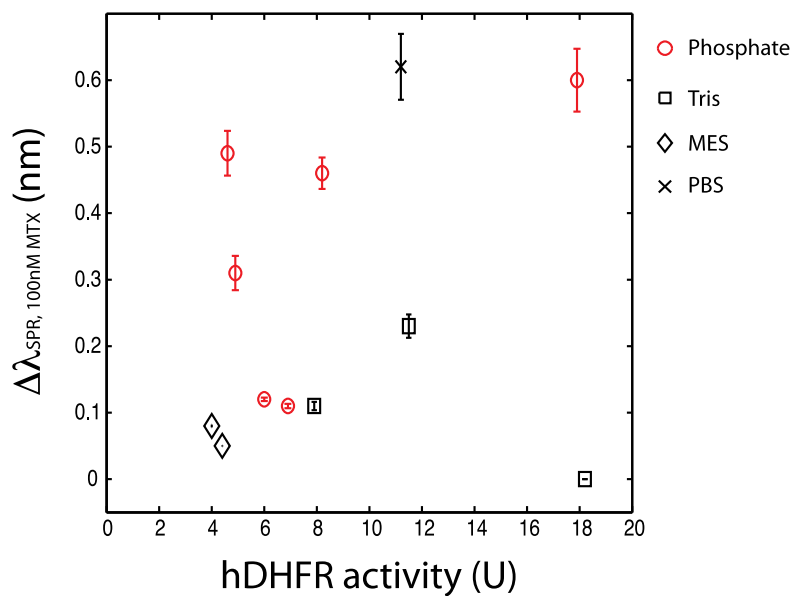


Figure SI1. The SPR response for 100 nM MTX is uncorrelated to the activity of hDHFR ($r^2 = 0.05$).

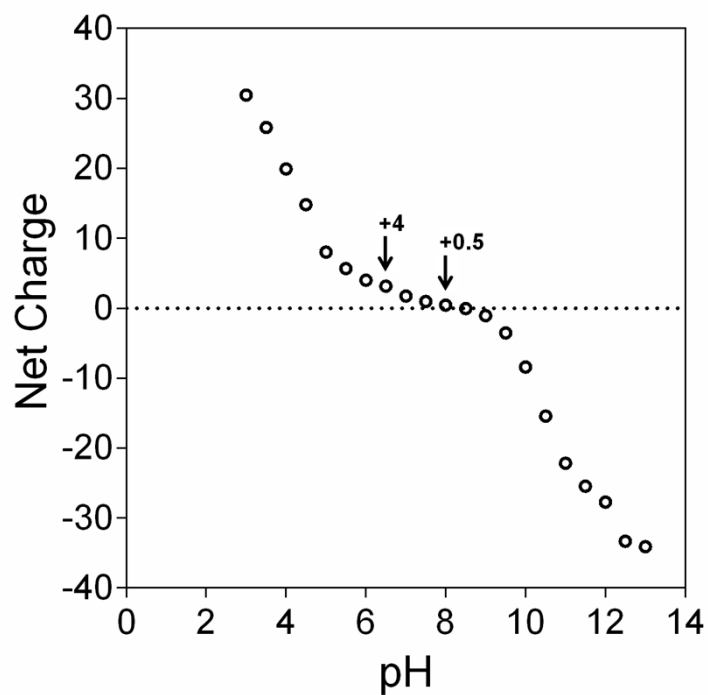


Figure SI2. Titration curve for hDHFR. Based on the simulated titration, a net charge (formal charge) of +4 is calculated at pH 6, and +0.5 at pH 8.

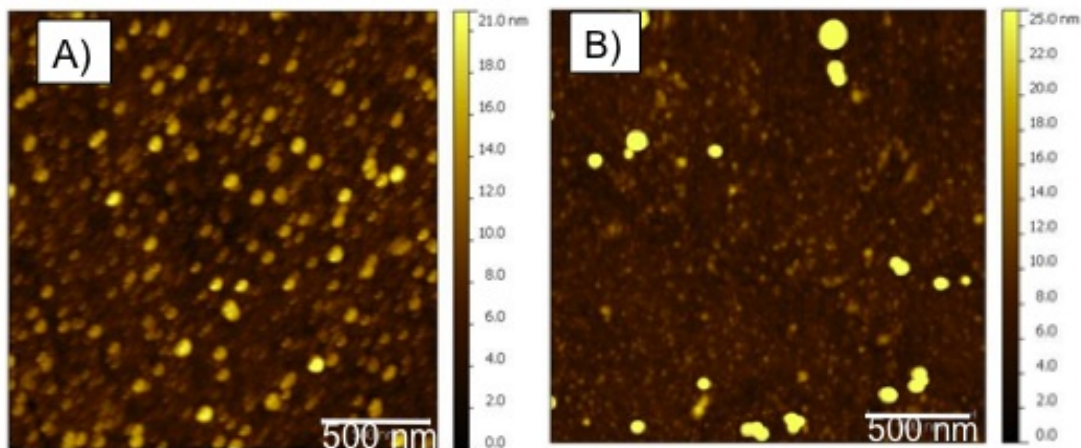


Figure SI3. AFM images were acquired for SPR sensors exposed to 0 (panel A) and 100 nM (panel B) MTX in the presence of folate anion Au NP. A) The surface is mainly covered with isolated Au NP with little evidence of aggregated Au NP. The surface concentration of Au NP is high for 0 nM MTX. B) The concentration of Au NP decreases significantly as expected in the presence of 100 nM MTX. There are a few occurrences of closely located Au NP, which may be due to aggregation or to a random coincidence of co-localized Au NP on different hDHFRs. The height of the Au NP (20-30 nm) measured by AFM is in good agreement with their size (23 nm). Folic acid Au NP were suspended in PBS with 10% FBS. AFM images were obtained in tapping mode with a Multimode microscope and a Nanoscope III controller (Digital Instruments) using the Nanoscope V5.30 software, operated under ambient atmosphere. The tips (Arrows NC model; spring constant 42 N/m, oscillation frequency 285 kHz, tip radius <10 nm) were obtained from Nanoworld (Neuchatel.Switzerland).

References

1. Volpato, J. P.; Yachnin, B. J.; Blanchet, J.; Guerrero, V.; Poulin, L.; Fossati, E.; Berghuis, A. M.; Pelletier, J. N., Multiple conformers in active site of human dihydrofolate reductase F31R/Q35E Double Mutant Suggest Structural Basis for Methotrexate Resistance. *Journal of Biological Chemistry* **2009**, *284* (30), 20079-20089.
2. Turkevich, J.; Stevenson, P. C.; Hillier, J., A study of the nucleation and growth processes in the synthesis of colloidal gold. *Discussions of the Faraday Society* **1951**, *11*, 55-75.
3. Haiss, W.; Thanh, N. T.; Aveyard, J.; Fernig, D. G., Determination of size and concentration of gold nanoparticles from UV-vis spectra. *Analytical Chemistry* **2007**, *79* (11), 4215-4221.
4. Zhao, S. S.; Bichelberger, M. A.; Colin, D. Y.; Robitaille, R.; Pelletier, J. N.; Masson, J.-F., Monitoring methotrexate in clinical samples from cancer patients during chemotherapy with a LSPR-based competitive sensor. *Analyst* **2012**, *137* (20), 4742-4750.
5. Bolduc, O. R.; Live, L. S.; Masson, J. F., High-resolution surface plasmon resonance sensors based on a dove prism. *Talanta* **2009**, *77* (5), 1680-1687.
6. Bolduc, O. R.; Lambert-Lanteigne, P.; Colin, D. Y.; Zhao, S. S.; Proulx, C.; Boeglin, D.; Lubell, W. D.; Pelletier, J. N.; Fethiere, J.; Ong, H.; Masson, J.-F., Modified peptide monolayer binding His-tagged biomolecules for small ligand screening with SPR biosensors. *Analyst* **2011**, *136* (15), 3142-3148.
7. Fogolari, F.; Brigo, A.; Molinari, H., The Poisson-Boltzmann equation for biomolecular electrostatics: a tool for structural biology. *J. Mol. Recognit* **2002** (15) 377-392.
8. Li, H.; Robertson, A. D.; Jensen, J. H., Very fast empirical prediction and rationalization of protein pKa values. *Proteins* **2005**, *61*, 704-721